TWO-PHASE JET RELEASES AND DROPLET DISPERSION: SCALED AND LARGE-SCALE EXPERIMENTS, DROPLET-SIZE CORRELATION DEVELOPMENT AND MODEL VALIDATION

Henk W.M. Witlox[1], Mike Harper[1], Adeyemi Oke[1], Phil J. Bowen[2], Peter Kay[2], Didier Jamois[3] and Christophe Proust[3]
[1]DNV Software, London, UK
[2]Cardiff University, Wales, UK
[3]INERIS, France

Many accidents involve two-phase releases of hazardous chemicals into the atmosphere. This paper describes the results of a third phase of a Joint Industry Project (JIP) on liquid jets and two-phase droplet dispersion. The aim of the project is to increase the understanding of the behaviour of sub-cooled non-flashing and superheated flashing liquid jets, and to improve the prediction of droplet atomisation, droplet dispersion and rainout.

Phase III of the JIP first included scaled experiments for materials with a range of volatilities (water, cyclohexane, butane, propane and gasoline). These experiments were carried out by Cardiff University including measurements of flow rate and initial droplet size across the full relevant range of superheats. Furthermore large-scale butane experiments were carried out by INERIS (France) to ensure that for more realistic scenarios the derived droplet size correlations are accurate.

Model validation and model improvements were carried out by DNV Software, including validation of release rate and initial droplet size against the above scaled and large-scale experiments. New refined correlations for droplet size distribution and Sauter Mean Diameter (SMD) were formulated and implemented into the Phast discharge model. These were compared against a range of other droplet size and rainout correlations published in the literature, in conjunction with validation against an extensive set of experiments. It was shown that the new droplet size correlation agrees better against experimental data than the existing Phast correlation. To further improve the rainout prediction, the Phast dispersion model (UDM) was also extended to allow simultaneous modelling of a range of droplet sizes and distributed rainout (rather than rainout at one point).

INTRODUCTION

Many accidents involve two-phase releases of hazardous chemicals into the atmosphere. Rainout results in reduced concentrations in the remaining cloud, but can also lead to extended cloud duration because of re-evaporation of the rained-out liquid. For accurate hazard assessment one must accurately predict both the amount of rainout and re-evaporation of the pool.

This paper describes the results of a third phase of a Joint Industry Project (JIP) on liquid jets and two-phase droplet dispersion. The aim of the project is to increase the understanding of the behaviour of sub-cooled (non-flashing) and superheated (flashing) liquid jets, and to improve the prediction of release rate, droplet atomisation, droplet dispersion and rainout.

Phase I of the JIP was carried out by Witlox and Bowen (2002) and involved a detailed literature review on flashing liquid jets and two-phase droplet dispersion. It served to establish the state of the art and provide recommendations for subsequent JIP work. The review considered models and validation data for the sub-processes of droplet atomisation, atmospheric expansion to ambient pressure, two-phase droplet dispersion, rainout, pool formation and re-evaporation; see Figure 1. The key issue identified was the lack of a justifiable and validated droplet atomisation model and furthermore limited experiments were found to be available for releases with significant rainout.

As a result, Phase II of the JIP was initiated. First scaled water experiments were carried out from low-superheat non-flashing jets to high-superheat fully flashing jets (Cleary et al., 2007). The experiments measured velocity and droplet size distribution close to the orifice (post-expansion data) in order to derive an improved droplet size correlation valid for release conditions. A criterion was derived for the transition between 'low' and 'high' superheat (non-flashing jets and fully flashing jets), and droplet atomisation correlations were proposed in the regimes for non-flashing (mechanical break-up), transition to flashing and fully flashing. The Phase II JIP droplet size correlation was compared with previous correlations from the literature (Witlox et al., 2007). This also included detailed validation for both initial droplet size and rainout.

Phase II was limited to scaled experiments for water with initial droplet-size data measured at a single value of the superheat only. Furthermore the modelling simplistically assumed one single averaged droplet size (Sauter Mean Diameter, SMD) with rainout at a single point only. As a result, Phase III was initiated to account for these issues. The current paper provides an overview of the Phase III results.

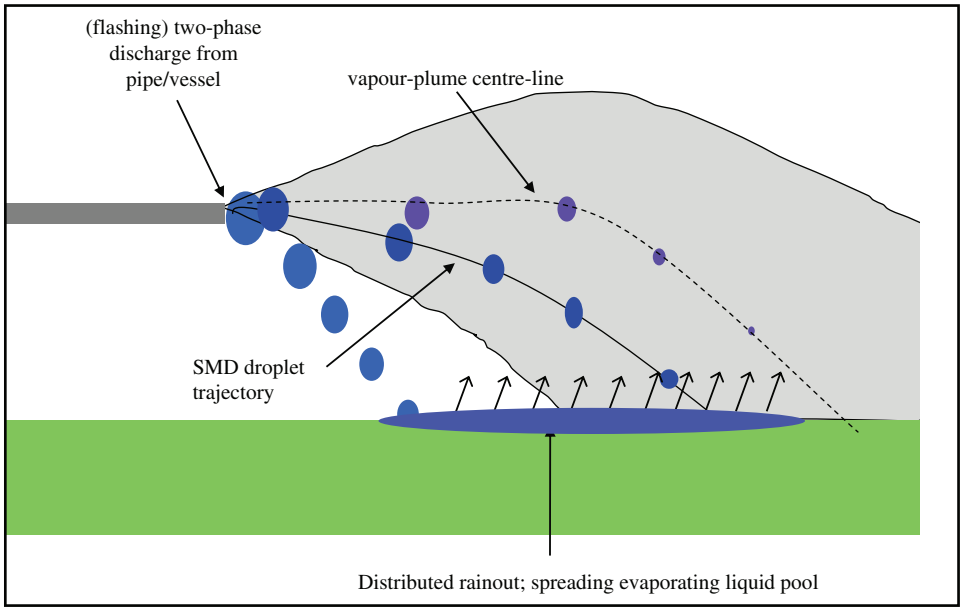

Figure 1. Modelling of droplet dispersion, distributed rainout and re-evaporation

Section 2 describes Phase III results of additional scaled water experiments at Cardiff University including measurements of flow rate and initial droplet size across the full relevant range of superheats. It also describes scaled experiments for cyclohexane, butane, propane and gasoline at the Gas Turbine Research Centre (Cardiff University), which were carried out to ensure that the derived droplet size correlations are also valid for other chemicals than water. Section 3 includes Phase III results of large-scale butane experiments, which were carried out by INERIS (France) to ensure that for more realistic scenarios the derived droplet size correlations are accurate.

Section 4 includes Phase III results of model validation and model improvements carried out by DNV Software, including validation of release rate and initial droplet size against the above scaled and large-scale experiments. A new refined correlation for droplet SMD is formulated and implemented into the discharge model in the hazard analysis package Phast. It is compared against a range of other droplet size and rainout correlations published in the literature, in conjunction with validation against an extensive set of experiments. It is shown that the new droplet size correlation agrees better against experimental data than the existing CCPS/Weber correlation used in Phast. To further improve the rainout prediction, the Phast dispersion model (UDM) was also extended to allow simultaneous modelling of a range of droplet sizes and distributed rainout (Figure 1) rather than rainout at one point. It also included further improvements to pool and dispersion modelling after rainout, and validation for dispersion from LNG and LPG pools.

SCALED EXPERIMENTS AND DEVELOPMENT OF DROPLET-SIZE CORRELATIONS

The first stage of Phase III of the JIP included scaled experiments for compounds with a range of volatilities at ambient conditions, i.e. water, gasoline, cyclohexane, butane and propane. These experiments were carried out by Cardiff University including measurements of flow rate and droplet size across the full relevant range of superheats. It also included the refinement of droplet size correlations in the regimes of mechanical break-up, transition to flashing, and fully flashing.

Droplet size measurements were taken using new advanced Phase Doppler Anemometry (PDA) technology for dense sprays recently acquired by Cardiff University. Unlike Phase II where data were provided for a single value of the superheat only, the new superheated spray rig allowed measurements to be taken across the entire relevant range of superheats with droplets measured in the range of 0-2132 μm, with a resolution of 0.02 μm. The rig consisted of a sealed pressure vessel with a helical-shaped electric incoloy heating element to heat the fluid inside the tank to a pre-determined 'stagnation temperature'. The fluid in the tank was pressurised with nitrogen. As the fluid is released the orifice temperature increases from ambient to near stagnation temperature. As the orifice temperature increases the jet break-up mechanism progresses through the full range of break-up regimes, from mechanical break-up to full flashing. Droplet data were recorded at 250 to 1000 mm downstream of the exit orifice depending on release condition and fluid. The mass flow rate was determined from the change in mass of the rig with time. Pressure and temperature were recorded 15 mm upstream of the exit orifice.

Table 1. Test matrix for scaled experiments (Cardiff University)

Fluid	Release condition	Stagnation temperature (°C)	Nozzle diameter (mm)	L/d_o (−)	Pressure (barg)
Water	Sub-cooled	Atmospheric	1, 2	1.01, 0.505	6, 10, 14
Cyclohexane	Sub-cooled	Atmospheric	0.75, 1, 2	1.4, 1.01, 0.505	6, 8, 10, 12, 14
Gasoline	Sub-cooled	Atmospheric	0.75, 1	4.53, 3.4	6, 8, 10, 12, 14
Water	Superheated	185	0.75, 1	3.54, 4.5	10
Cyclohexane	Superheated	180	1, 2	1.01, 0.505	7.5, 10
Butane	Superheated	Atmospheric	0.75, 1, 2	1.4, 1.01, 0.5	9.5, 8, 7.5
Propane	Superheated	Atmospheric	1, 2	1.01, 0.5	6.5, 7.5
Gasoline	Superheated	180	1	1.01	10

First additional experiments were carried out for water including variation of superheat in order to further validate and possibly improve the SMD correlation as a function of superheat. Subsequently further experiments were carried out for non-aqueous compounds (hydrocarbons) in order to ensure that the derived droplet size correlations are also valid for other chemicals (including fine-tuning of the correlation). These experiments involved cyclohexane and butane experiments, and up to a limited extent also gasoline and commercial propane. Table 1 includes a test matrix for the Phase III scaled experiments. This table indicates the test fluid, the type of experiment (sub-cooled; or superheated, where the orifice temperature T_o varies between ambient and stagnation temperature), the nozzle diameter d_o, the ratio of nozzle length L and d_o, and the pressure immediately upstream of the orifice.

Droplet size data for the sub-cooled experiments were recorded 500 mm down-stream (see Figure 2); this was with the exception for the 0.75 mm cyclohexane data which was recorded 1000 mm down-stream due to large break-up length. Data for the sub-cooled releases were recorded at 11 radial positions from +10 mm to −10 mm in 2 mm steps. Data for the transient flashing experiments were recorded 250 mm down-steam (considered a good compromise between sub-cooled and fully flashing break-up lengths) and at one radial position on the centre line.

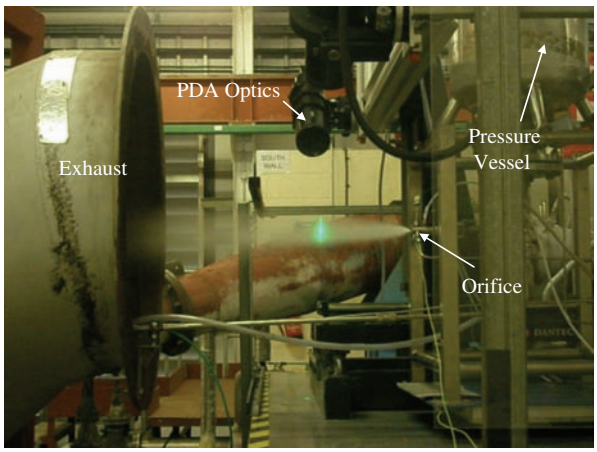

Figure 2. PDA droplet size measurement for scaled cyclohexane experiment (Cardiff University)

The development of the new Phase III correlations for SMD and droplet size distribution was based on a best fit of experimental data for water and cyclohexane. The new correlation as illustrated by Figure 3 retains the tri-functional shape of SMD as function of superheat $\Delta\theta_{sh}$ (K) (including regimes for mechanical break-up, transition to flashing, and fully flashing), as was initially proposed by Phase II and confirmed by Figure 4a. However it now includes considerable further fine-tuning accounting for the larger droplet sizes measured by the new PDA system and also accounting for possibly larger droplets not being measured ('clipping of data') as shown in Figure 5.

Figure 3 defines three subsequent regimes of mechanical break-up (prior to point A), transition to flashing (between point A and point B) and fully-flashing (after Point B). Major changes for the Phase III JIP correlation compared to the Phase II JIP correlation include a new SMD correlation for the first regime of mechanical break-up, a slight modification of regime transition criteria (valid between points A and B), and a new SMD proposed for the fully flashed condition (valid after point B).

The SMD correlation for mechanical break-up valid for the first regime prior to point A defines the non-dimensionalised SMD (SMD/d_o) as a function of the aspect ratio (L/d_o), the liquid Reynolds number Re_{Lo}, and the liquid Weber number We_{Lo},

$$\frac{SMD}{d_o} = F\left[We_{Lo}, \mathrm{Re}_{Lo}, \frac{L}{d_o}, \frac{\mu_{Lo}}{\mu_{water,stp}}, \frac{\sigma_{Lo}}{\sigma_{water,stp}}, \frac{\rho_{Lo}}{\rho_{water,stp}}\right]$$
$$= 74\, We_{Lo}^{-0.85}\, \mathrm{Re}_{Lo}^{0.44}\left(\frac{L}{d_o}\right)^{0.114}\left(\frac{\mu_{Lo}}{\mu_{water,stp}}\right)^{0.97}\left(\frac{\sigma_{Lo}}{\sigma_{water,stp}}\right)^{-0.37}$$
$$\times\left(\frac{\rho_{Lo}}{\rho_{water,stp}}\right)^{-0.11} \quad (1)$$

Here Re_{Lo} and We_{Lo} are representative of orifice (exit) conditions, i.e. nozzle diameter d_0, orifice velocity u_0, liquid surface tension σ_{Lo}, liquid dynamic viscosity μ_{Lo}, liquid

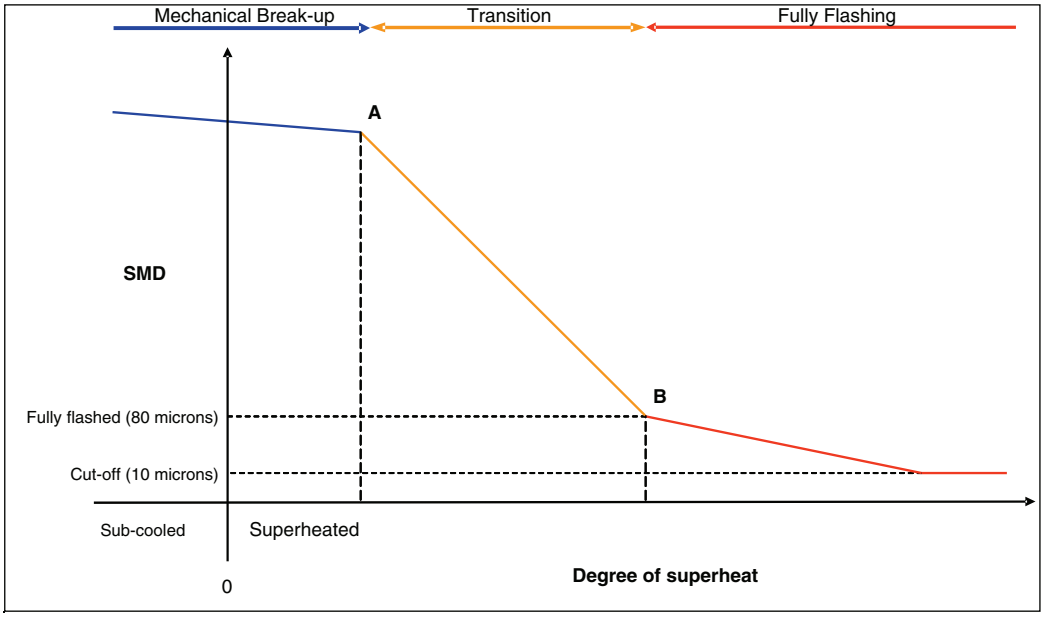

Figure 3. Tri-functional curve for Sauter Mean Diameter (SMD) as function of superheat

density ρ_{Lo} (all evaluated at the orifice temperature T_0). Furthermore the subscript water,stp indicates properties of water taken at standard temperature and pressure (1 atmosphere and 0 °C). For $L/d_o < 0.1$ and $L/d_o > 50$ the cut-off values $L/d_o = 0.1$ and $L/d_o = 50$ are applied. The release is modelled as a meta-stable liquid, with a solid liquid core at the exit of the orifice.

The definition of criteria for transition between regimes (Points A and B) is based on the thermodynamic properties of the liquid (Jakob number Ja) and the ratio of inertia forces to surface tension forces in the spray (vapour Weber number We_v). In order to permit similarity scaling for use of the transition criteria with other liquids the Jakob number is modified by a correction factor (ϕ) as defined by Kitamura et al. (1986), based on the liquid to vapour density ratio. The transition points A and B are defined by

$$\text{Point A:} \quad Ja\,\phi = 48\ We_v^{-\frac{1}{7}}, \quad with\ \phi = 1 - e^{-2300\left(\frac{\rho_v}{\rho_L}\right)} \tag{2}$$

$$\text{Point B:} \quad Ja\,\phi = 108\ We_v^{-\frac{1}{7}} \tag{3}$$

where ρ_v and ρ_L are the vapour and liquid density evaluated at the orifice temperature T_o. In accordance with the paper by Kitumura, the vapour Weber number We_v and the

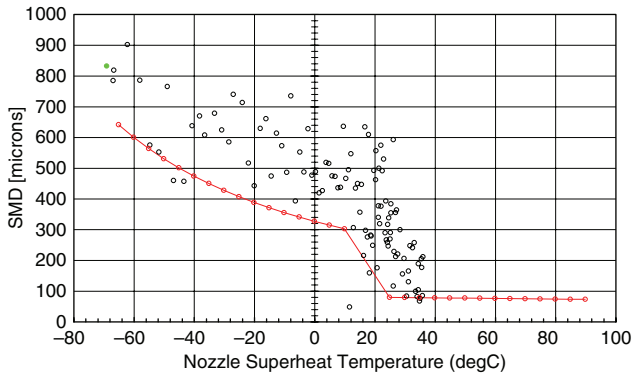

(a) SMD: experimental data and Phase III correlation

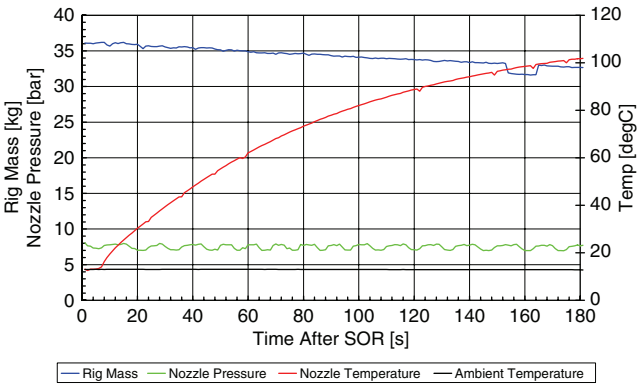

(b) rig mass, orifice pressure and temperature

Figure 4. Measured data for cyclohexane jet (1 mm orifice size)

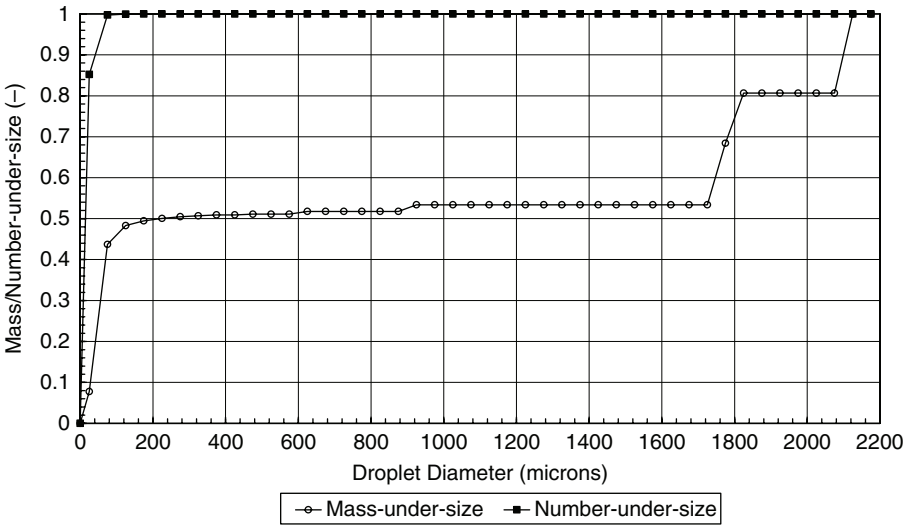

(a) flashing jet (2 mm, $L/d_o = 0.5$, P = 10 barg)

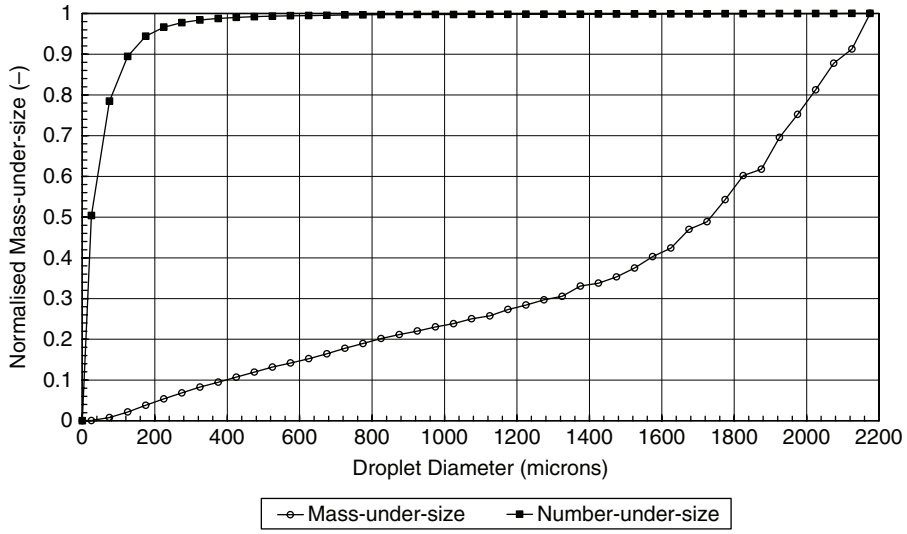

(b) sub-cooled jet (2 mm, $L/d_o = 0.5$, P = 10 barg)

Figure 5. Droplet size distribution data for cyclohexane jet (2 mm orifice)

Jacob number Ja are evaluated as

$$We_v = \frac{\rho_v u_o^2 d_o}{\sigma_{Lo}},\ Ja = \frac{C_{pL}\Delta T_{sh}}{h_{fg}}\frac{\rho_L}{\rho_v} \tag{4}$$

Here C_{pL} is the specific heat of the liquid (J/kg/K), and h_{fg} the latent heat of evaporation (J/kg), both evaluated at the orifice temperature.

The fully flashing SMD (Point B) is assumed to occur at 80 μm, after which it is assumed to decrease at a constant rate (0.1 μm/K) until the SMD reaches a final nominal constant value (10 μm).

One very important objective of this Phase III programme is to substantiate the model structure and underlying philosophy summarized in Figure 3. The transient scatter plots generated, as exemplified in Figure 4a, provide confidence in pursuing and refining this trifunctional approach to modeling superheated fluid releases.

Figure 4 includes the transient SMD against temperature for a cyclohexane jet along with rig temperature/pressure/mass. This figure very clearly illustrates the rapid decay of SMD at around 20 degrees superheat (onset of flashing).

Figure 5 includes droplet size distribution data for both sub-cooled and flashing cyclohexane jets represented as mass-under-size and number-under-size plots. The number-under-size plots for both the sub-cooled and fully flashing jet show that it appears that all the data has been recorded. However, the mass-under-size plots show that it

Table 2. Test matrix for large-scale butane experiments (INERIS)

Number of experiment	Orifice diameter (mm)	Release pressure (barg)	Release temperature (C)	PDA axial distances (cm)	PDA resolution d_{max} (μm)
1	5	6	15–26	60	700
2	10	6	26–27	60, 85	800
3	10	10	19–22	60, 85	800
4	15	6	17–21	60, 85	750
5	10	6	9–10	40, 60, 85	750
6	10	2	7–9	40, 60, 85	750

appears that some data has been clipped particularly for the non-flashing jet. This is due to limitations in the droplet sizing technique, i.e. for some cases there are possibly droplets larger than those actually measured.

Future publications are planned to include further details of the above experiments and the new correlations for SMD droplet size and droplet size distribution.

LARGE-SCALE BUTANE EXPERIMENTS

The second stage of Phase III included large-scale butane experiments by INERIS. These were carried out to ensure that for more realistic scenarios the derived droplet size correlations are accurate. Both flow rate and droplet-size measurements were carried out.

Six experiments were carried out using butane of purity 99.5%. Table 2 includes the corresponding test matrix. It is seen that the experiments include a range of orifice sizes (5, 10 and 15 mm), release pressures (2, 6 and 10 barg), and superheats (7–27 °C). Measurements taken include ambient data (temperature, pressure), tank data (weight, pressure and temperature as function of time), data immediately upstream of the orifice (pressure and temperature as function of time) and PDA droplet size measurements. Table 2 includes the axial distances at which data were taken at a range of crosswind distances (0, ±3, ±6 cm). It also includes the maximum droplet size d_{max} that could be measured. This was considered to be a sufficient range for the distribution of number of droplets, but larger droplets may be missed resulting in a possibly inaccurate droplet volume distribution.

Figure 6 illustrates the experimental rig and PDA droplet size measurements for one of the large-scale butane experiments. Figure 7 includes the droplet size distribution data for one of the INERIS experiments. Like for the Cardiff experiments, it is observed that some data may be 'clipped', i.e. for some cases there are possibly droplets larger than those actually measured.

MODEL IMPLEMENTATION AND VALIDATION

The third stage of Phase III included the implementation and validation of the recommended droplet size correlations and droplet size distribution into extended versions of the discharge and dispersion models present in the consequence modelling package "Phast" and the risk package "Phast Risk". It also included validation of the Phast discharge model DISC, and improved logic in the Phast dispersion model UDM for distributed rainout and the re-evaporation and dispersion of rained out liquid.

Figure 6. PDA droplet size measurement for large-scale butane jet experiment (INERIS)

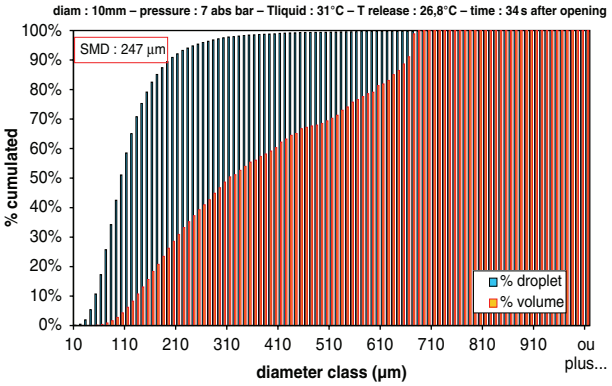

Figure 7. Droplet size distribution data for INERIS experiment 2 (10 mm orifice, 6 barg, 26.8°C)

Improvement and Validation of Discharge Model (Flow Rate and Droplet Size)

First a literature survey was carried out to establish a sufficient comprehensive verification and validation dataset for the Phast models for modelling discharge from orifices and line ruptures. Subsequently verification and validation was carried out for the flow rate for the short pipeline rupture and orifice discharge models included in DISC. This included verification against the analytical Bernoulli equation for incompressible liquids, verification of the default Phast discharge model (including compressible effects) against the reservoir simulation package PRO-II and validation against published experiments for orifice and pipe releases for water, propane and butane.

Subsequently the discharge model was extended to include implementation of two new SMD droplet size correlations, which included a droplet size correlation by Melhem et al. (1995), as well as the new Phase III JIP correlation described above.

Along with other experimental data available from the literature, simulated flow rate and droplet size results from the discharge model were validated against the above scaled Cardiff experiments (water, cyclohexane, butane, propane and gasoline) and the large-scale INERIS butane experiments. Flow rate was overall found to be well within 20% of measured data, which is considered to be very good given the accuracy of the flow rate measurements. See Figure 4 for validation of the Phase III JIP correlation against one of the cyclohexane experiments.

Figure 8 illustrates that the improved droplet size correlation agrees much better with the new Phase III experimental data than the previous Phast correlation. This

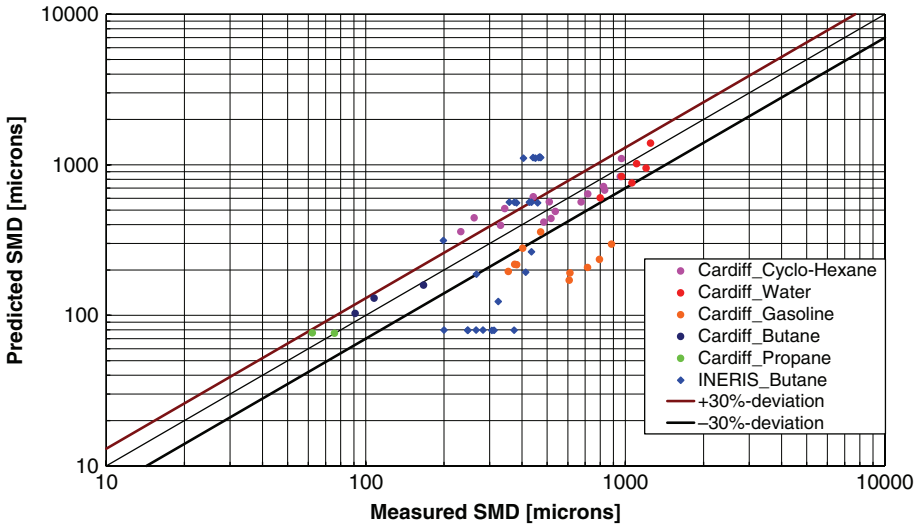

(a) New Phase III JIP SMD correlation

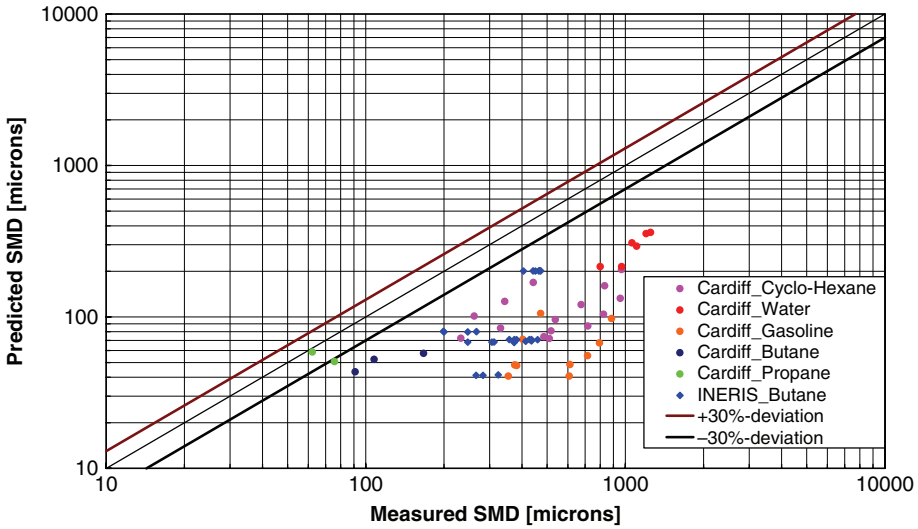

(b) Current Phast 6.531/6.54 SMD correlation

Figure 8. Validation of SMD droplet size correlation against Phase III experiments

is also true for other experiments available from the literature. The old Phast correlation generally under-predicts since it erroneously advices to apply the minimum of its mechanical droplet-size correlation (based on Weber correlation) and its flashing droplet size correlation (based on CCPS correlation).

Improvement and Validation of Dispersion Model (Pool/Cloud Linking and Distributed Rainout)

The UDM outdoor dispersion model in Phast allows for two-phase dispersion including droplet modelling, rainout of the droplets to form a pool, PVAP pool evaporation calculations and subsequent addition of vapour back to the cloud.

As part of the Phase III work, improvements were carried out to pool/dispersion modelling after rainout (improved dispersion logic and validation from a pool). The UDM model was also extended to allow for modelling of droplet size distribution (droplet parcels) and distributed rainout.

The UDM model has been improved to include the robust modelling of rainout and re-evaporation. It includes a more consistent modelling of re-evaporation directly from a pool source, or after a rained out pool has been left behind by a residual vapour cloud. These two scenarios now use the same sub-model, whereas previously pool sources were simplistically modelled as low-velocity vertical jets starting from the pool. The improved model starts dispersing at the upwind edge of the pool, with pool vapour being added while the cloud is travelling above the pool, and better reflects the geometry of the dispersing cloud in the vicinity of the pool. The new logic has been validated against experiments for dispersion from liquid evaporating pools (LNG and LPG – Burro, Coyote and Maplin Sands experiments) as well as for dispersion from vapour area sources (CO_2 – Kit Fox experiments), and improved predictions have been obtained.

In the current Phast model (version 6.5) the starting condition of the UDM is a single droplet size defined by the value of the SMD droplet size immediately following expansion to ambient; droplet equations are solved for this SMD droplet size only. As part of the current work the current UDM droplet logic is extended to allow for a range of droplet sizes and therefore distributed rainout; see Figure 1. In the UDM model the initial droplet distribution is split into a number of equal-mass droplet parcels, and for each droplet parcel droplet equations are solved. The larger droplets rain out at a shorter distance, while the smaller droplets evaporate before they reach the ground. This predicts rainout distributed in the along-wind direction and is expected to give more accurate rainout predictions. The extended Phast discharge and dispersion models (DISC, UDM) have been validated against the CCPS experiments and give an improved fit compared to the current Phast correlation.

Future publications are planned to include details of the above discharge and dispersion model improvements and associated model validation.

FUTURE WORK

The Phase III work included the further refinement of initial droplet size correlations and the development of a new methodology to predict distributed rainout. The objective of a Phase IV project, now underway, is to generate experimental data for non-flashing experiments to validate this new methodology, and to make model refinements where necessary. The scope of the project involves rainout experiments for a non-volatile fuel by HSL laboratories including variation of stagnation pressure, orifice size, and weather conditions. Measurements taken will include ambient data, release data (flow rate), initial droplet size distribution, dispersion data (concentrations up to the point of rainout), and distributed rainout data. The droplet size measurements will be undertaken utilising direct imaging techniques, and as such Phase IV will enable studies of the influence of non-spherical particles known to exist particularly for sub-cooled releases, which the PDA technique would not be able to resolve. The Phase IV experimental work will be combined with model validation by DNV (of flow rate, initial droplet size distribution, concentrations, and distributed rainout) using the new Phase III rainout formulation. This may also include further model improvement where deemed to be necessary.

It is the intention to make the new Phase III droplet size correlation available in Phast 6.6, and the Phase IV distributed rainout model in a subsequent version of Phast.

Following Phase IV, further additional work may be considered involving rainout experiments for flashing jets. Also further model improvements and model validation are required for multi-component releases.

CONCLUSIONS

1. A refined empirical sub-model for predicting droplet size and droplet size distributions from non-flashing and flashing jet releases has been proposed based on a best fit against scaled water and cyclohexane experiments. The tri-functional droplet size correlation proposed previously has been shown to be credible, and covers the regimes of mechanical break-up, transition between non-flashing and flashing, and fully flashing jets.
2. Alongside a range of other droplet size correlations, the new droplet-size correlation has been implemented into new versions of consequence models in the hazard-analysis package Phast and the risk analysis package Phast Risk (discharge model DISC, atmospheric expansion model ATEX and Unified Dispersion Model, UDM).
3. A detailed validation has been carried out for the discharge model DISC. This includes validation of both the flow rate (with accuracy typically well within 20%) and the droplet size against both experiments carried out as part of the current Phase III of the JIP (scaled water, cyclohexane, butane, propane and gasoline experiments by Cardiff University and large-scale

butane experiments by INERIS), as well as other experiments available in the literature. Overall, the new droplet size correlation shows better agreement with experimental data compared with the previous droplet size correlation.

4. A new methodology has been developed to model distributed rainout. Phase IV of the JIP has recently commenced to further validate this new methodology by means of a number of rainout experiments for non-flashing jets.

ACKNOWLEDGEMENTS

Financial support of the work reported in this paper (Phase III project) was provided by DNV Software, Gaz de France, RIVM (Dutch Government), TOTAL, Norske Hydro and Statoil (now merged into StatoilHydro). The contents of this paper including any opinions and/or conclusions expressed, are those of the authors alone and do not necessarily reflect the policy of these organisations.

REFERENCES

Cleary, V.M., Bowen, P.J. and Witlox, H.W.M., 2007, "Flashing liquid jets and two-phase droplet dispersion, I. Experiments for derivation of droplet atomisation correlations", *Journal Hazardous Materials*, 142: 786–796.

Kitamura Y., Morimitsu H. and Takahashi T., 1986, "Critical Superheat for Flashing of Superheated Liquid Jets" *Ind. Eng. Chem Fundamentals*, Vol. 25, No. 2: 207–211.

Melhem, G.A., Comey, K.R. and Gustafson, R.M., 1995, "The TEXACO/UOP HF Alkylation Additive Technology: aerosolization reduction effects", *Proceedings of Int. Conf. and Workshop on Modelling and Mitigating the consequences of accidental releases of hazardous materials*, AIChE/CCPS, September 26–29.

Witlox, H.W.M. and Bowen, P.J., 2002, "Flashing liquid jets and two-phase dispersion – A review", Work carried out by DNV for HSE, Exxon-Mobil and ICI Eutech, *HSE Books*, Contract research report 403/2001.

Witlox, H.W.M., Harper, M., Bowen, P.J. and Cleary, V.M., 2007, "Flashing liquid jets and two-phase dispersion – II. Comparison and validation of droplet size and rainout formulations", *Journal of Hazardous Materials*, 142: 797–809.